Original Article

The Anterolateral Triangle: Implications for a Transnasal Prelacrimal Approach to the Floor of the Middle Cranial Fossa

American Journal of Rhinology & Allergy
2020, Vol. 34(5) 671–678
© The Author(s) 2020
Article reuse guidelines:
sagepub.com/journals-permissions
DOI: 10.1177/1945892420922757
journals.sagepub.com/home/ajr
SAGE

Lifeng Li, MD[1,2], Nyall R. London Jr, MD, PhD[2,3,4], Daniel M. Prevedello, MD[2,5], and Ricardo L. Carrau, MD, MBA[2,5]

Abstract

Background: The anterolateral triangle enclosed by the foramen rotundum and foramen ovale constitutes part of the floor of the middle cranial fossa (MCF).

Objective: To assess the feasibility of a transnasal prelacrimal approach for accessing the floor of MCF via an anterolateral triangle corridor and to determine the extent of maximal exposure while safeguarding neurovascular structures.

Methods: A transnasal prelacrimal approach was performed in 5 cadaveric specimens (10 sides). Following the identification of foramen rotundum and foramen ovale, the bony ridge between 2 was drilled to expose the MCF. The temporal lobe dura was then elevated laterally, and the distances from foramen ovale to the respective borders of the area of the MCF window were measured using a surgical navigation device.

Results: The MCF was exposed with a 0° scope in all specimens also exposing significant landmarks including the middle meningeal artery, greater superficial petrosal nerve, superior petrous sinus, and arcuate eminence. Average distances from foramen ovale to the anterior, posterior, and lateral exposed borders were 22.86 ± 1.87 mm, 27.24 ± 0.94 mm, and 24.23 ± 1.61 mm, respectively. The average area of exposed MCF window was 554.12 ± 60.22 mm^2. Preservation of vidian nerve, greater palatine nerve, lateral nasal wall, and nasolacrimal duct was possible in all 10 sides.

Conclusion: It is feasible to access the floor of MCF via an endoscopic transnasal prelacrimal approach with seemingly low risk.

Keywords

anterolateral triangle, prelacrimal approach, foramen rotundum, foramen ovale, middle cranial fossa

Introduction

In the past 3 decades, endonasal expanded approaches (EEA) have provided access for selected lesions in the skull base of the anterior, middle and posterior fossae, as well as the craniovertebral junction.[1–3] As a representative paradigm, the endonasal transpterygoid approach was successfully adopted to address lesions arising from the lateral recess of the sphenoid sinus and the anteromedial aspect of Meckel's cave.[4,5]

The anterolateral triangle is enclosed by foramen rotundum and foramen ovale constituting part of the floor of middle cranial fossa (MCF).[2,3] Traditional approaches to resect lesions in this region include the anterolateral and lateral open craniotomies.[6,7] Their potential for damaging the temporalis muscle and the need for retraction of the temporal lobe have fostered

[1]Department of Otolaryngology—Head and Neck Surgery, Beijing Tongren Hospital, Capital Medical University, Beijing, China
[2]Department of Otolaryngology—Head and Neck Surgery, The James Cancer Hospital at the Wexner Medical Center of The Ohio State University, Columbus, Ohio
[3]Department of Otolaryngology—Head and Neck Surgery, Johns Hopkins School of Medicine, Baltimore, Maryland
[4]Sinonasal and Skull Base Tumor Program, National Institute on Deafness and Other Communication Disorders, National Institutes of Health, Bethesda, Maryland
[5]Department of Neurological Surgery, The James Cancer Hospital at the Wexner Medical Center of The Ohio State University, Columbus, Ohio

Corresponding Author:
Ricardo L. Carrau, Department of Otolaryngology—Head and Neck Surgery, The Ohio State University Wexner Medical Center, Starling Loving Hall—Room B221, 320 West 10th Avenue, Columbus, OH 43210, USA.
Email: Ricaro.carrau@osumc.edu

the development of other minimally invasive techniques.[8] During the past decade, other minimal access techniques (ie, transorbital approach,[9] transantral, and modified EEA techniques[10,11]) to the floor of MCF have emerged.

Using EEA, Wong[10] described that access to the MCF through a transpterygoid approach could be achieved and combined with transposition of the infraorbital nerve to increase its exposure. In this study, the lateral nasal wall was resected and the vidian neurovascular bundle was sacrificed to enhance exposure. Moreover, a transantral approach to the MCF, to provide visualization and access to the MCF, also has been described.[11] However, its need for a sublabial incision, and resection of the anterior and posterior maxillary walls may lead to post-operative complications such as damage to facial soft tissues, infraorbital nerve dysfunction, oroantral fistula, and infections due to the introduction of oral flora into the field.[11]

The transnasal prelacrimal approach was originally described by Zhou et al. to address lesions located in the prelacrimal recess of maxillary sinus.[12] A prelacrimal approach could also provide direct access to address lesions adjacent or involving the foramen rotundum and foramen ovale or their corresponding neurovascular bundles.[13,14] Moreover, previous cadaveric studies demonstrated that a transnasal prelacrimal approach, with preservation of lateral nasal wall, nasolacrimal duct, and neurovascular bundles in pterygopalatine fossa, is a less invasive technique than both the transpterygoid EEA and the transantral approach.[15–17] We therefore hypothesized that in order to decrease the associated comorbidities, the floor of MCF could be accessed via a transnasal prelacrimal approach.

The purpose of this study was to assess the feasibility of a transnasal prelacrimal approach for accessing the floor of MCF via an anterolateral triangle corridor. Moreover, it also aimed to determine the extent of maximal exposure while preserving the safety of neurovascular structures.

Materials and Methods

An endoscopic transnasal prelacrimal approach to the MCF was performed in 5 adult cadaveric specimens (10 sides) at the Anatomy Laboratory Toward Visuospatial Surgical Innovations in Otolaryngology and Neurosurgery (ALT-VISION) at the Wexner Medical Center of the Ohio State University. Authors involved in the dissections were certified by local regulatory agencies dealing with the use of human tissues and cadaveric studies in The Ohio State University. Major vessels of the neck, including the common carotid and vertebral arteries and the internal jugular vein were commercially injected with red (artery) and blue (vein) latex dyes. All the specimens were preserved in 70% alcohol.

A 0° scope (4-mm diameter, 18-cm length) coupled to a high definition camera and monitor and endoscopic dissecting instruments (Karl Storz Endoscopy, Tuttlingen, Germany) were used to provide visualization and complete the dissections. A high-speed drill (Stryker Co., Kalamazoo, Michigan) with straight handed-piece and 3 to 4 mm rough diamond (hybrid) burrs was used for the dissection and removal of bony structures. An AIDA system (Karl Storz Endoscopy) was used to record and save images (TIFF format) and videos (MPEG format). Still photographs and videos were obtained to define and document the anatomic relationships from the endoscopic perspective to be correlated with the multiplanar computed tomography (CT) views provided by the image guidance system (Stryker Co.).

Each specimen underwent high resolution CT scanning and their Digital Imaging and Communications in Medicine (DICOM) format images data were imported to a Stryker surgical navigation system (Stryker Co.). Measurements including the distances from foramen ovale to the anterior, lateral, and posterior exposed borders of the MCF, the areas of bony prelacrimal window and MCF window were performed using the navigation system. Results are presented as the mean $\pm$ standard deviation (SD).

Results

Surgical Technique

The technical nuances of transnasal prelacrimal approach has been previously described,[15–17] its main steps include:

(i) A vertical mucoperiosteal incision on the lateral wall of the nasal cavity, between the pyriform aperture and anterior head of the inferior turbinate, extending inferiorly to the nasal floor.
(ii) Removal of the bony attachment of inferior turbinate with a high-speed drill to expose the nasolacrimal duct and enter into the maxillary sinus anterolateral to the nasolacrimal duct.
(iii) Displacement of the nasolacrimal duct medially and partial removal of the medial and anterior walls of maxillary sinus to increase instrument maneuverability.

Through the prelacrimal window, the posterolateral wall of the maxillary sinus was removed with a Kerrison rongeur to expose the periosteum. The infraorbital nerve was traced proximally to the maxillary nerve (V_2) at the inferior orbital fissure. Following removal of the periosteum, the internal maxillary artery and its distal branches were identified (Figure 1(A)) and sacrificed to expose the lateral pterygoid muscle and greater wing of the sphenoid (Figure 1(B)). Subperiosteal dissection of the superior head of lateral

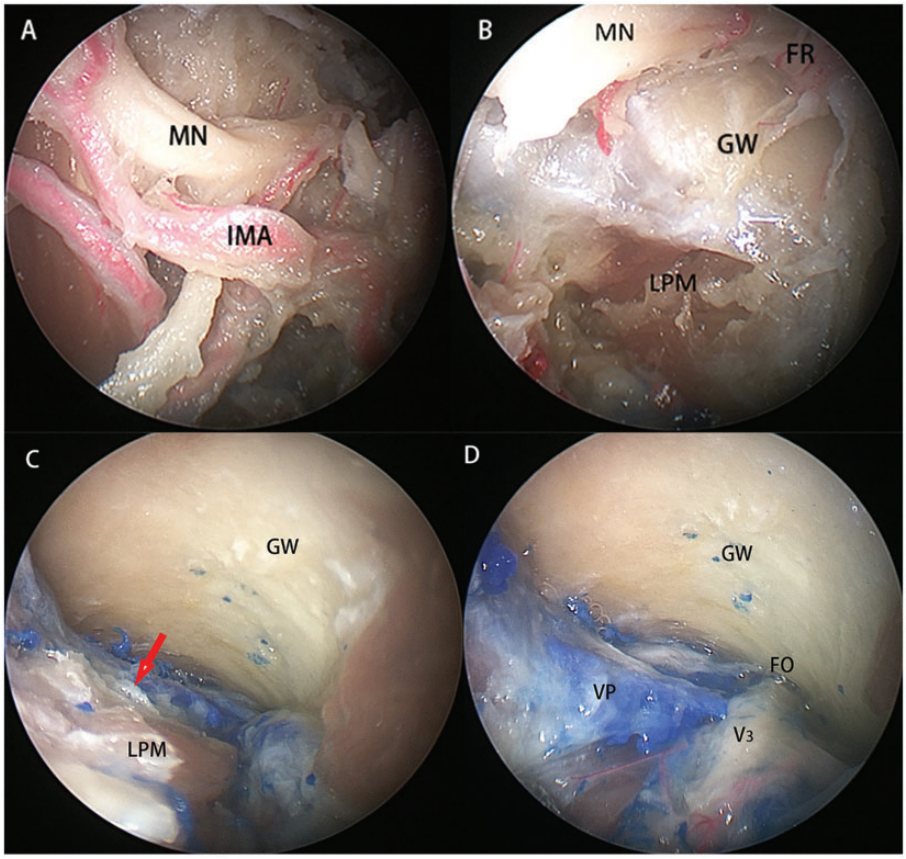

Figure 1. The IMA on right side was resected to increase the exposure (A); the MN was traced backward to identify FR and GW of the sphenoid (B); the LPM was elevated under the periosteum (C, arrow); the VP was protected by the periosteum (D, arrow). FO, foramen ovale; FR, foramen rotundum; GW, greater wing; IMA, internal maxillary artery; MN, maxillary nerve; LPM, lateral pterygoid muscle; VP, venous plexus.

pterygoid muscle allowed its inferolateral displacement, away from the greater wing of the sphenoid, to expose foramen ovale (Figure 1(C)). Staying in a subperiosteal plane minimizes the injury to the pterygoid vascular plexus and thus would minimize bleeding in a clinical scenario (Figure 1(D)).

The bony ridge of the anterolateral triangle enclosed between the foramen rotundum and foramen ovale (Figure 2(A)) was drilled to expose the dura of the MCF (Figure 2(B)). The anterior and lateral walls of the lateral recess of sphenoid sinus (if present) were also removed to increase the access corridor (Figure 2 (C)). As one elevates the dura beneath the temporal lobe, the lateral aspect of Meckel's cave (with V_1–V_3 and the Gasserian ganglion) could be exposed (Figure 3).

At the floor of MCF, the middle meningeal artery emerges from the foramen spinosum and could be identified posterolateral to the foramen ovale (Figure 4(A)). The middle meningeal artery courses in a lateral direction and branches out to supply the greater superficial petrosal nerve (GSPN; Figure 4(B)). After further elevation of the dura, the GSPN, arcuate eminence, superior petrous sinus, and posterior petrous edge could also be identified in the posterolateral direction (Figure 5).

Navigational Measurements

In 7 of 10 sides (70%), superior displacement of the maxillary nerve was needed to increase the exposure of greater wing of the sphenoid and the foramen rotundum.

Three of the 10 sides (30%) had a well-pneumatized lateral recess of sphenoid sinus, in which case its lateral wall constituted the medial border of the MCF (Figure 2(C)).

Average distances from the foramen ovale to the anterior, posterior, and lateral exposed borders of MCF (Figure 6) were 22.86 ± 1.87 mm, 27.24 ± 0.94 mm and 24.23 ± 1.61 mm, respectively (Table 1); the average area of the expanded prelacrimal window and MCF window (Figure 2(B), enclosed dot lines) was 441.84 ± 37.75 mm^2 and 554.12 ± 60.22 mm^2, respectively (Table 2).

Discussion

By comparison with the endoscopic transpterygoid approach to expose the MCF as previously reported,[10]

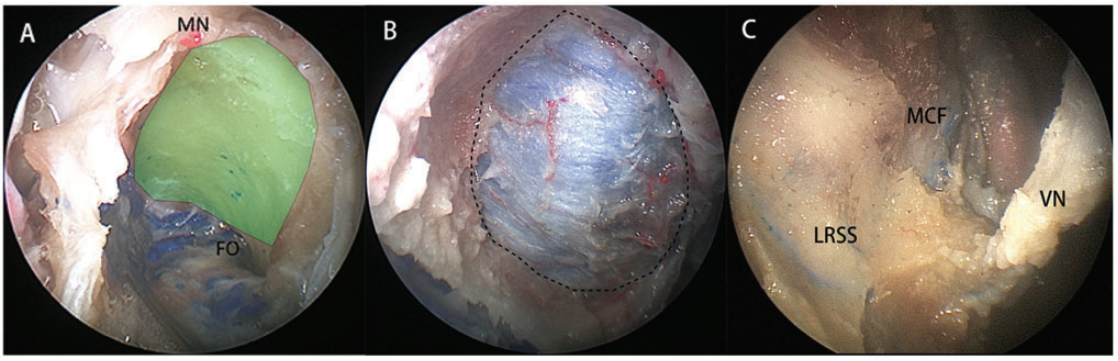

Figure 2. The bone ridge (A, highlighted) enclosed between FR and FO on right side was drilled to expose the window of the middle cranial fossa (B, dotted lines); the anterior wall of LRSS was removed to increase exposure (C). FO, foramen ovale; LRSS, lateral recess of sphenoidal sinus; MCF, middle cranial fossa; MN, maxillary nerve; VN, vidian nerve.

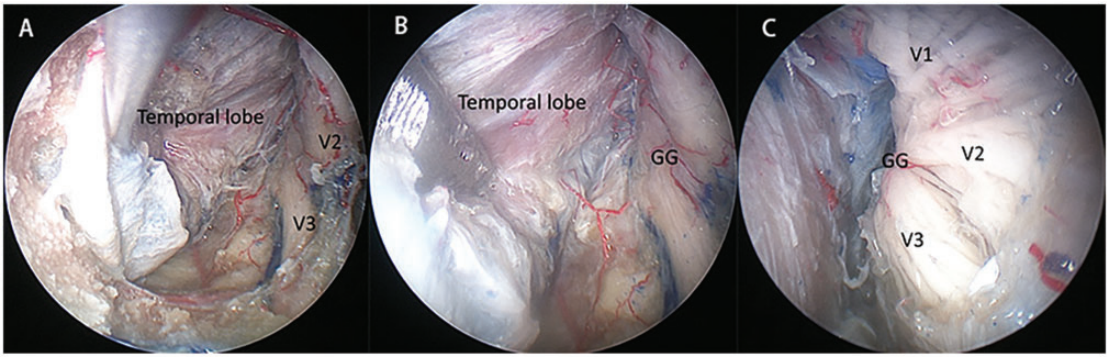

Figure 3. The dura of temporal lobe on right side was separated and elevated from the Meckel's cave (A) to expose the GG and V_1, V_2, and V_3 (B and C). GG, Gasserian ganglion.

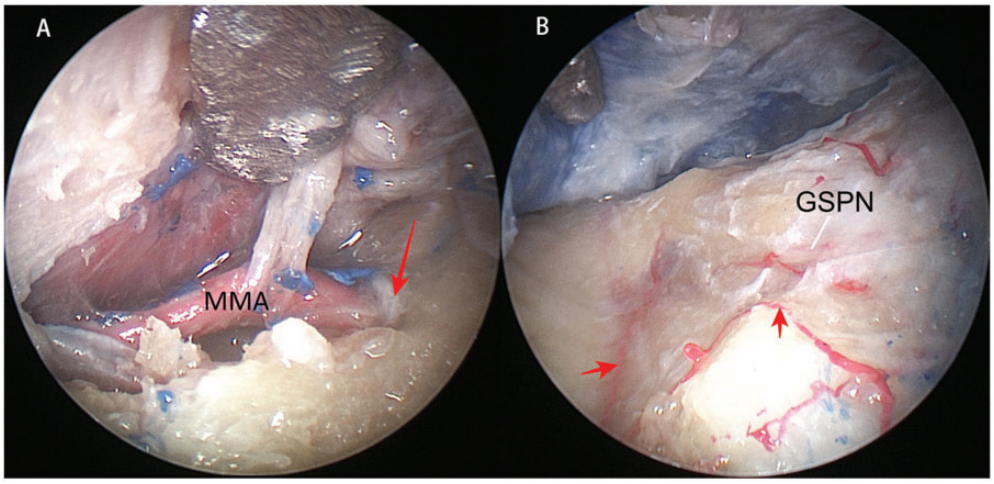

Figure 4. The MMA on right side exits the foramen spinosum (A, arrow) and coursed laterally in the middle cranial fossa floor providing some small branches to nurture the GSPN (B, arrow). GSPN, greater superficial petrosal nerve; MMA, middle meningeal artery.

the transnasal prelacrimal approach spares the lateral nasal wall, nasolacrimal duct, and the greater palatine, and vidian nerves in pterygopalatine fossa.[18] Preservation of the lateral nasal wall may reduce postoperative nasal morbidity and the preservation of neurovascular contents in the pterygopalatine fossa may also decrease the incidence of palatal numbness and xerophthalmia.[19]

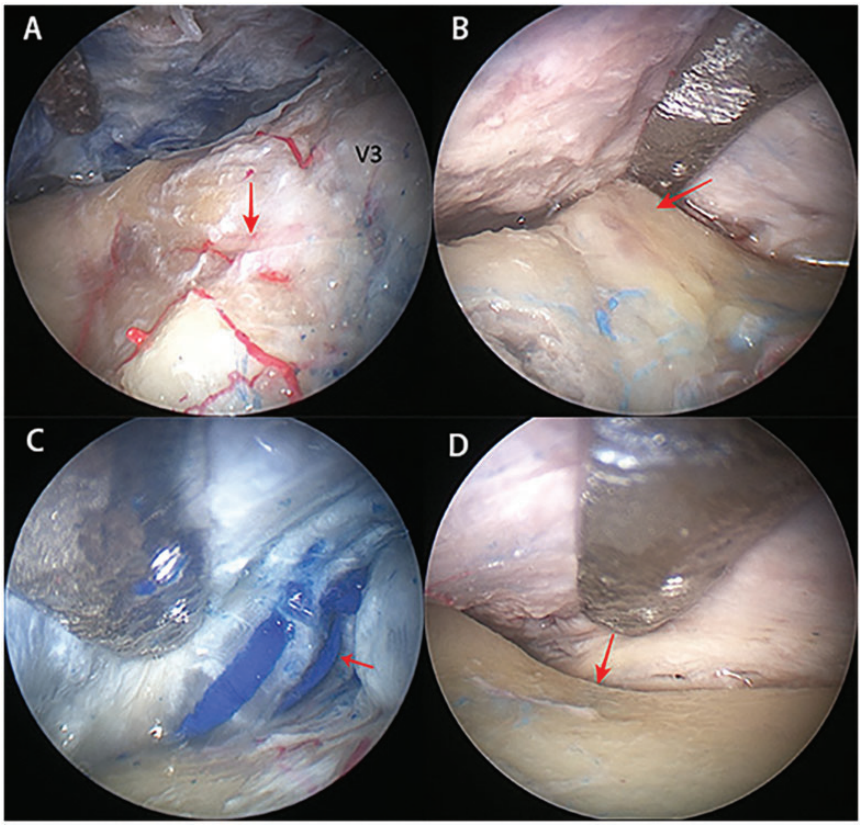

Figure 5. The GSPN (A, arrow), arcuate eminence (B, arrow), superior petrous sinus (C, arrow), and posterior edge of the petrous apex on right side (D, arrow) could be identified at the floor of middle cranial fossa.

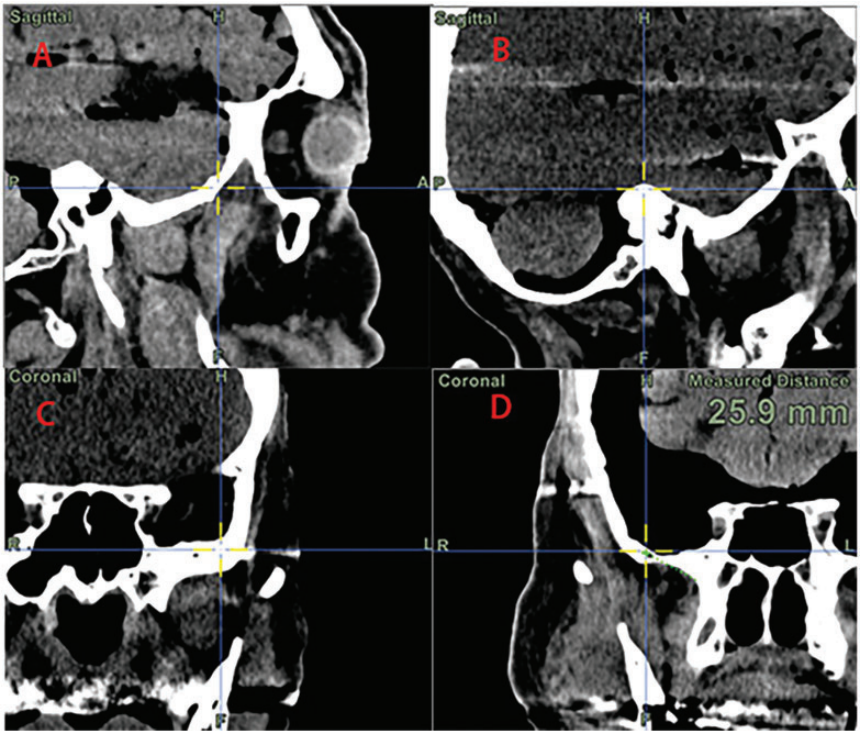

Figure 6. The most anterior (A), posterior (B), and lateral (C) exposed borders accessed by a prelacrimal approach were recorded, and the distances from foramen ovale to these borders were measured with navigation system (D).

Table 1. Measurement of Distances (mm) From FO to LB, PB, and AB of the Expanded Middle Cranial Fossa.

No.	FO to LB	FO to PB	FO to AB
1	22.70	28.20	21.40
2	25.00	28.30	21.20
3	22.60	27.60	25.90
4	25.70	28.70	21.20
5	23.20	27.40	22.80
6	21.80	26.10	21.00
7	26.60	26.90	24.90
8	24.20	26.40	25.40
9	25.90	26.60	22.60
10	24.60	26.20	22.20
Mean±SD	24.23 ± 1.61	27.24 ± 0.94	22.86 ± 1.87

Abbreviations: AB, anterior border; FO, foramen ovale; LB, lateral border; PB, posterior border.

Table 2. Areas (mm^2) of the Bony Prelacrimal Window and the Middle Cranial Fossa Window.

No.	Bony Prelacrimal Window	Middle Cranial Fossa Window
1	384.48	485.78
2	410.26	530.00
3	435.12	585.34
4	495.90	544.84
5	438.47	528.96
6	462.00	457.80
7	491.31	662.34
8	416.16	614.68
9	474.33	585.34
10	410.40	546.12
Mean±SD	441.84 ± 37.75	554.12 ± 60.22

Both the foramen rotundum and foramen ovale could be sufficiently exposed via a transnasal prelacrimal approach.[12–17] Therefore, the distal aspect of the anterolateral triangle, which is enclosed by V_2 (foramen rotundum) and V_3 (foramen ovale), providing a direct avenue and the rationality for exposure of the floor of MCF via a prelacrimal approach.[5] The average area of the MCF window was 554.12 ± 60.22 mm^2, which was adequate for maneuverability into the floor of MCF through this corridor. However, the drilling of the floor of MCF via an endonasal corridor may carry the risk of injury to the V_2, V_3, and the dura of MCF.

Foramen ovale is also an important landmark to locate the internal carotid artery and Eustachian tube, the petrous and paraclival segments of the internal carotid artery, as well as the Eustachian tube are lying posterior to it.[20–22] Since all bone drilling for exposure of MCF via a prelacrimal approach was lateral and anterior to the foramen ovale, the risk of damage to the internal carotid artery and Eustachian tube is minimal. A transterygoid EEA, progressing in a medial to lateral direction; however, it carries a greater risk of damaging these structures.[4,23] Furthermore, a significant venous bleeding from the pterygoid venous plexus and cavernous sinus will be anticipated for procedures around the floor of MCF. Therefore, a subperiosteal manipulation and strategies for hemostasis (eg, gelatin sponge, fluid gelatin) should be adequately prepared before performing a procedure close to the floor of the MCF and the Meckel's cave.

In addition to the foramen rotundum and foramen ovale,[20] this study also suggests that the middle meningeal artery, which is consistently located posterolateral to the foramen ovale, may serve as an additional landmark for identification of neurovascular structures within the MCF.[24] Of note, accessing the lateral aspect of Meckel's cave does not require sacrifice of the middle meningeal artery. Addressing lesions in the posterolateral aspect of the MCF, however, require sacrificing the middle meningeal artery for adequate exposure. Based on the measurement presented in this study, the resection of the middle meningeal artery can enhance the lateral exposure of the MCF to 24.23 ± 1.61 mm away from the foramen ovale via a transnasal prelacrimal corridor.

GSPN travels from the geniculate ganglion to the posterior aspect of V_3 crossing the floor of MCF, then combines with the deep petrous nerve to form the vidian nerve.[25] GSPN is a useful landmark for surgical procedures in the MCF[26] and also seems to serve this purpose during an endonasal prelacrimal approach. Other landmarks such as the arcuate eminence and posterior petrous ridge could also be exposed via a prelacrimal approach; however, one should recognize that the contraction of the brain in a cadaveric specimen eases their exposure, which could be much more difficult in a patient. For management of lesions in the posterolateral aspect of the MCF; however, significant retraction of the temporal lobe seems unavoidable; thus, the anterolateral or lateral craniotomies are still the golden standard to access lesions in this area.[6,7,27]

Reconstruction of the MCF defect is an important consideration before selecting a surgical approach. As a component of multilayer skull base reconstruction (2 layers of facia lata inside), we recommend transposition of an ipsilateral posterior pedicled lateral nasal wall flap or a contralateral pedicled nasoseptal flap for overlay reconstruction of deficiency of the MCF, the utility and efficacy of these flaps have been illustrated previously.[28,29]

Despite the average area of the bony prelacrimal window was 441.84 ± 37.75 mm^2 after partial removal of the medial and anterior walls of the maxillary sinus, the authors recognized that it was still a challenge to simultaneously manipulate the rod-lens endoscope and 2 instruments through the prelacrimal window.[16]

The addition of an anterior antrostomy such as a Caldwell–Luc approach or any other variant, including expanding the prelacrimal window laterally, could obviate the restriction for instrumentation.[30] However, removal of the piriform crest and anterior face of the maxillary sinus, and displacement of the nasolacrimal duct as required to facilitate or expand the prelacrimal corridor, may carry the risk of postoperative piriform aperture stenosis, alar constriction, and epiphora. Moreover, for cases with hypoplasia of the maxillary sinus or poor pneumatization of the prelacrimal fossa where the distance between the pyriform aperture and nasolacrimal duct may be smaller than usual, utilization of a transnasal prelacrimal corridor may be difficult or impossible.[12,15] Therefore, this reiterates the need to study the radiological anatomy preoperatively to determine the suitability of the approach.

Through the cadaveric investigations performed in the present study, it seems that the transnasal prelacrimal approach can provide an alternative or as an assistance for open craniotomies for management of lesions arising from the floor of MCF with seemingly low risks. However, it is still a preclinical study, which deserves further clinical validation. Nonetheless, the investigation of associated landmarks and the anatomical basis are sound.

Conclusion

A transnasal prelacrimal approach is feasible to access the floor of MCF via an anterolateral triangle corridor. Risks of damaging the internal carotid artery and Eustachian tube are low, and structures such as the lateral nasal wall, vidian nerve, and greater palatine nerve may be preserved.

Declaration of Conflicting Interests

The author(s) declared the following potential conflicts of interest with respect to the research, authorship, and/or publication of this article: N. R. L. holds stock in Navigen Pharmaceuticals and was a consultant for Cooltech Inc., neither of which are relevant to this manuscript. The other authors declare no potential conflicts of interest.

Funding

The author(s) received no financial support for the research, authorship, and/or publication of this article.

ORCID iD

Lifeng Li https://orcid.org/0000-0002-0114-7608

References

1. Kassam A, Snyderman CH, Mintz A, Gardner P, Carrau RL. Expanded endonasal approach: the rostrocaudal axis. Part II. Posterior clinoids to the foramen magnum. *Neurosurg Focus*. 2005;19:E4.
2. Kassam AB, Gardner P, Snyderman C, Mintz A, Carrau R. Expanded endonasal approach: fully endoscopic, completely transnasal approach to the middle third of the clivus, petrous bone, middle cranial fossa, and infratemporal fossa. *Neurosurg Focus*. 2005;19:E6.
3. Kassam AB, Snyderman C, Gardner P, Carrau R, Spiro R. The expanded endonasal approach: a fully endoscopic transnasal approach and resection of the odontoid process: technical case report. *Neurosurgery*. 2005;57:E213; discussion E213.
4. Kasemsiri P, Solares CA, Carrau RL, et al. Endoscopic endonasal transpterygoid approaches: anatomical landmarks for planning the surgical corridor. *Laryngoscope*. 2013;123:811–815.
5. Kassam AB, Prevedello DM, Carrau RL, et al. The front door to Meckel's cave: an anteromedial corridor via expanded endoscopic endonasal approach—technical considerations and clinical series. *Neurosurgery*. 2009;64: ons71–ons82; discussion ons82–ons73.
6. Klironomos G, Dehdashti AR. Orbitozygomatic craniotomy and trans-sylvian approach for resection of a tuberculum sella meningioma with extension to the posterior fossa. *Neurosurg Focus*. 2017;43:V13.
7. Pontius AT, Ducic Y. Extended orbitozygomatic approach to the skull base to improve access to the cavernous sinus and optic chiasm. *Otolaryngol Head Neck Surg*. 2004;130:519–525.
8. Goel A. Extended lateral subtemporal approach for petroclival meningiomas: report of experience with 24 cases. *Br J Neurosurg*. 1999;13:270–275.
9. Jeon C, Hong CK, Woo KI, et al. Endoscopic transorbital surgery for Meckel's cave and middle cranial fossa tumors: surgical technique and early results. *J Neurosurg*. 2018;131:1126–1135.
10. Wong RH. Endoscopic endonasal transrotundum middle fossa exposure: technique of transpterygoid maxillary nerve transposition. *World Neurosurg*. 2018;112:131–137.
11. Truong HQ, Sun X, Celtikci E, et al. Endoscopic anterior transmaxillary "transalisphenoid" approach to Meckel's cave and the middle cranial fossa: an anatomical study and clinical application. *J Neurosurg*. 2018;130:227–237.
12. Zhou B, Han DM, Cui SJ, Huang Q, Wang CS. Intranasal endoscopic prelacrimal recess approach to maxillary sinus. *Chin Med J (Engl)*. 2013;126:1276–1280.
13. Gao L, Zhou L, Dai Z, Huang X. The endoscopic prelacrimal recess approach to the pterygopalatine fossa and infratemporal fossa. *J Craniofac Surg*. 2017;28:1589–1593.
14. Zhou B, Huang Q, Shen PH, et al. The intranasal endoscopic removal of Schwannoma of the pterygopalatine and infratemporal fossae via the prelacrimal recess approach. *J Neurosurg*. 2016;124:1068–1073.
15. Li L, London NR Jr, Prevedello DM, Carrau RL. Anatomical variants of the infraorbital canal: implications for the prelacrimal approach to the orbital floor. *Am J Rhinol Allergy*. 2020;34(2):176–182.
16. Li L, London NR Jr, Silva S, Prevedello D, Carrau RL. Transnasal prelacrimal approach to the inferior intraconal

space: a feasibility study. *Int Forum Allergy Rhinol*. 2019;9:1063–1068.
17. Li L, London NR Jr, Prevedello DM, Carrau RL. Endoscopic prelacrimal approach to lateral recess of sphenoid sinus: feasibility study. *Int Forum Allergy Rhinol*. 2020;10:103–109.
18. Hosseini SM, Razfar A, Carrau RL, et al. Endonasal transpterygoid approach to the infratemporal fossa: correlation of endoscopic and multiplanar CT anatomy. *Head Neck*. 2012;34:313–320.
19. McLaughlin N, Bresson D, Ditzel Filho LF, et al. Vidian nerve neurofibroma removed via a transpterygoid approach. *Minim Invasive Neurosurg*. 2011;54:250–252.
20. Li L, London NR Jr, Prevedello DM, Carrau RL. Anatomy based corridors to the infratemporal fossa: Implications for endoscopic approaches. *Head Neck*. 2020;42:846–853.
21. Mehta GU, Raza SM. Endoscopic endonasal transpterygoid approach to petrous pathologies: technique, limitations and alternative approaches. *J Neurosurg Sci*. 2018;62:339–346.
22. Freeman JL, Sampath R, Quattlebaum SC, et al. Expanding the endoscopic transpterygoid corridor to the petroclival region: anatomical study and volumetric comparative analysis. *J Neurosurg*. 2018;128:1855–1864.
23. Al-Nashar IS, Carrau RL, Herrera A, Snyderman CH. Endoscopic transnasal transpterygopalatine fossa approach to the lateral recess of the sphenoid sinus. *Laryngoscope*. 2004;114:528–532.
24. Carrillo JF, Rivas Leon B, Celis MA, Ponce-de-Leon S, Ochoa-Carrillo FJ. Anterolateral and lateral skull-base approaches for treatment of neoplastic diseases. *Am J Otolaryngol*. 2004;25:58–67.
25. Osawa S, Rhoton AL Jr, Seker A, Shimizu S, Fujii K, Kassam AB. Microsurgical and endoscopic anatomy of the vidian canal. *Neurosurgery*. 2009;64:385–411; discussion 411–382.
26. Tanriover N, Sanus GZ, Ulu MO, et al. Middle fossa approach: microsurgical anatomy and surgical technique from the neurosurgical perspective. *Surg Neurol*. 2009;71:586–596; discussion 596.
27. Campero A, Ajler P, Goldschmidt E, Rica C, Martins C, Rhoton A. Three-step anterolateral approaches to the skull base. *J Clin Neurosci*. 2014;21:1803–1807.
28. Hadad G, Bassagasteguy L, Carrau RL, et al. A novel reconstructive technique after endoscopic expanded endonasal approaches: vascular pedicle nasoseptal flap. *Laryngoscope*. 2006;116:1882–1886.
29. Rivera-Serrano CM, Bassagaisteguy LH, Hadad G, et al. Posterior pedicle lateral nasal wall flap: new reconstructive technique for large defects of the skull base. *Am J Rhinol Allergy*. 2011;25:e212–e216.
30. Lee JJ, Ryu G, Kim HY, Dhong HJ, Chung SK, Hong SD. Endoscopic two-port technique for infratemporal fossa tumors: using prelacrimal medial maxillectomy and Caldwell-Luc approach. *World Neurosurg*. 2019;124:56–61.